

DOI: 10.1002/adma.200602181

Electrophoresis Coating of Titanium Dioxide on Aligned Carbon Nanotubes for Controlled Syntheses of Photoelectronic Nanomaterials**

By Yaodong Yang, Liangti Qu, Liming Dai,* Tae-Sik Kang, and Michael Durrstock*

Owing to its excellent semiconducting and photoelectronic properties,^[1] TiO₂ has recently attracted a great deal of interest for a large variety of applications. Examples include the use of TiO₂ nanoparticles/films as photocatalysts for environment protection,^[2] photoelectron mediators for sensors,^[3] photosensitizers in light-emitting devices,^[4] and solar cells.^[5] With the recent development in nanoscience and nanotechnology, there is now a pressing need to integrate multicomponent nanoscale entities into multifunctional materials and devices.^[6] In this regard, TiO₂ nanoparticles have been deposited onto various catalytic supports to improve their photocatalytic activities.^[7] In particular, activated carbon fibers and spheres were used as a class of chemically stable mesoporous catalytic supports to provide multiple active sites and to allow effective diffusion of reactants for the photocatalytic reactions.^[8]

Because of their unique one-dimensional electronic structure, large surface area, good chemical and thermal stability, and excellent mechanical properties,^[9] carbon nanotubes (CNTs) may work better than other carbon forms to support TiO₂ for a wide range of applications, especially in photocatalytic and optoelectronic systems. As a consequence, some recent attempts have been made to coat nonaligned multiwalled CNTs with TiO₂ thin films,^[10] whilst several synthetic routes were devised to prepare nonaligned TiO₂ nanotubes,^[11] nanowires, or nanomembranes.^[12] It will be a significant advantage if we can coat vertically aligned CNTs (VACNTs) with TiO₂ as the coaxial structure should allow the nanotube framework to provide a good mechanical stability, high thermal/electrical conductivity, and large surface/interface area necessary for efficient optoelectronic and sensing devices.^[13] The alignment

structure will also facilitate surface modification for adding novel surface/interfacial characteristics to the TiO₂ and VACNT hybrids,^[14] and allow the constituent nanotube devices to be collectively addressed through a common substrate/electrode.^[15] We previously prepared various vertically aligned conducting polymer–CNT coaxial nanowires by electrochemically depositing a concentric layer of an appropriate conducting polymer onto the individual aligned CNTs for advanced biosensing applications.^[16] In this Communication, we report the use of VACNTs not only as the support for electrophoretic coating^[17] with TiO₂ but also as the template for producing aligned TiO₂ nanotubes and nanomembranes. The resultant aligned TiO₂–VACNT coaxial nanowires, TiO₂ nanotubes, and TiO₂ nanomembranes were demonstrated to possess novel photocurrent responses and photoinduced electron-transfer properties.

In a typical experiment, we prepared VACNTs by pyrolyzing iron(II) phthalocyanine (FePc) on a Si substrate according to our published procedures.^[18,19] For electrophoresis, a Si-supported VACNT film thus produced was used as the cathode and a graphite rod as the anode. Both electrodes were immersed in a sol–gel solution approximately 2 cm apart from each other. The sol–gel solution was prepared by dissolving titanium (IV) isopropoxide (10 mL) in 30 mL of ethanol containing glacial acetic acid (12 wt %), followed by the addition of 0.6 mL of HCl in deionized water (pH 2) under magnetic stirring for 1 h. A potential of 1 V was then applied between the two electrodes for several minutes to electrophoretically deposit the positively charged, protonated TiO₂ clusters^[20] onto the VACNT cathode. After the electrophoretic deposition, the samples were dried at 80 °C for 1 h. The chemical stoichiometry, crystal structure, and thickness of the resultant TiO₂ coating can be regulated by controlling the electrophoresis conditions (e.g. applied voltage, deposition time) and a post-electrophoresis heat treatment for crystallization and densification (typically, 500 °C in air for 20 min).

Figure 1a shows a typical scanning electron microscopy image of ca. 7 μm long VACNTs. The corresponding SEM image under higher magnification in Figure 1b shows an average diameter of ca. 50 nm for the as-synthesized CNTs. Upon electrophoresis, TiO₂ clusters were deposited on sidewalls of the VACNTs as nanoparticles (Fig. 1c). Further electrophoresis deposition up to ca. 30 min caused additional TiO₂ clusters to fill up the spaces between the pre-deposited TiO₂ nanoparticles, leading to the growth of a continuous TiO₂ coating along

[*] Prof. L. Dai, Y. Yang, Dr. L. Qu
Department of Chemical and Materials Engineering
School of Engineering, UDRI, University of Dayton
300 College Park
Dayton, OH 45469-0240 (USA)
E-mail: ldai@udayton.edu

Dr. M. Durrstock, Dr. T.-S. Kang
Materials and Manufacturing Directorate
Air Force Research Laboratory, AFRL/MLBP
Wright-Patterson AFB, OH 45433 (USA)
E-mail: michael.durrstock@wpafb.af.mil

[**] We thank AFOSR (FA9550-06-1-0384) and AFRL/ML for support. We are grateful to Dr. Jianwei Liu and Ms. Amanda Schrand for their help.

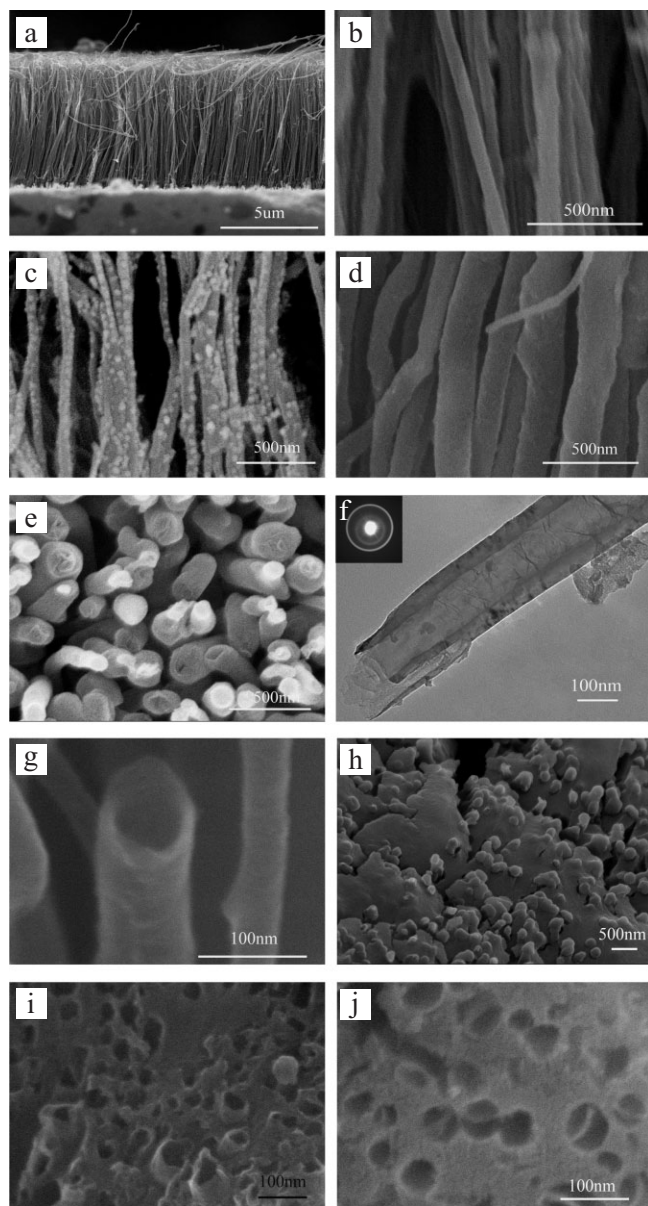


Figure 1. SEM images of a) the VACNTs (The misalignment seen for some of the CNTs was caused by the nanotube electrode preparation.), b) as for (a) under higher magnification. The corresponding SEM images for the VACNTs after the electrophoresis deposition of TiO₂ coating at 1 V for deposition times of c) 15 min and d) 30 min. e) Top view of the TiO₂-VACNT coaxial nanowires corresponding to (d) after heat treatment at 600 °C in air for 30 min. The sample has been turned over from the Si substrate to demonstrate the possibility of transferring the aligned nanowire array with full integrity. f) A TEM image of the resultant TiO₂-coated VACNTs shown in (d). The inset of (f) shows an electron diffraction pattern of the TiO₂ coating. SEM images of g) the sample corresponding to that in Figure 1e after thermal annealing at 600 °C in air for 2 h, showing vertically aligned TiO₂ hollow tubes after the removal of the VACNT template through air oxidation, h) VACNTs after a prolonged electrophoretic coating with TiO₂ at 1 V for 3 h, and i,j) the loosely and more densely packed TiO₂ membranes formed by annealing the corresponding TiO₂-infiltrated VACNT films at 600 °C in air for 2 h.

the whole nanotube length (Fig. 1d). Figure 1d shows similar features as the pristine VACNTs (Fig. 1b) but with a larger diameter (ca. 120 nm on average) due to the presence of the newly coated TiO₂ layer. A top-view SEM image of the sample corresponding to Figure 1d after the heat treatment at 600 °C in air for 30 min is given in Figure 1e, which clearly shows the vertically aligned coaxial nanowires of the CNTs sheathed with TiO₂ coating with some of the CNT cores having been removed by oxidation with air under the high temperature. Figure 1f shows a typical transmission electron microscopy (TEM) image taken at the tip region of the TiO₂-VACNT coaxial nanowires, showing a polycrystalline (inset of Fig. 1f) TiO₂ coating along the nanotube length. The thickness of the TiO₂ layer was determined from the TEM image to be ca. 30–40 nm, consistent with the SEM observations (see Fig. 1b and d).

By annealing the sample corresponding to Figure 1e at 600 °C in air for 2 h, most of the VACNT templates were removed through the air oxidation, leaving the TiO₂ hollow shells as aligned TiO₂ nanotubes (Fig. 1g). Prolonged electrophoretic deposition led to partially or fully infiltrating TiO₂ into the gaps between the constituent TiO₂-VACNTs coaxial nanowire, as exemplified by Figure 1h. Thermal annealing the partially or fully TiO₂-infiltrated VACNT films produced by the prolonged electrophoretic deposition resulted in the formation of either a loosely packed (Fig. 1i) or more densely packed (Fig. 1j) TiO₂ membrane.

X-ray photoelectron spectroscopy measurements revealed an O/Ti atomic ratio close to that of stoichiometric TiO₂. A Raman spectrum taken from the TiO₂-coated VACNT sample corresponding to Figure 1e shows a strong peak at 144 cm⁻¹ with three weaker peaks at 397, 518, and 639 cm⁻¹ (Fig. 2a), characteristic of the photoelectronically active TiO₂ anatase phase.^[21] The remaining two bands centered at 1380 and 1580 cm⁻¹ in Figure 2a are attributable to the D- and G-bands, respectively, of the underlying multiwalled CNTs.^[9] The corresponding X-ray diffraction (XRD) pattern in Figure 2b shows peaks at 25.35, 37.15, 37.90, 38.55, 48.15, 54.1, 55.1, 62.85, 69.1, 70.5, 75.3, and 83.15 °, once again, attributable to the TiO₂ anatase structure. The weak peak at 27.80 ° arises, most probably, from the Si substrate. No diffraction peak was seen for the rutile structure at 27.44 °.

The anatase phase of TiO₂ has a bandgap of ca. 3.2 eV, which could be considered as a wide-bandgap photoelectronic active semiconductor.^[22] Indeed, TiO₂ has been widely used as a class of photocatalysts for environmental protection by decomposing organisms with UV irradiation.^[23] Therefore, the newly prepared TiO₂-VACNT coaxial nanowires, TiO₂ nanotubes, and TiO₂ nanomembranes are expected to exhibit some new photoelectronic properties. In particular, the well-defined surface/interface structures between the TiO₂ and CNT phases and unique photoelectronic properties of the TiO₂-VACNT coaxial nanowires should provide important

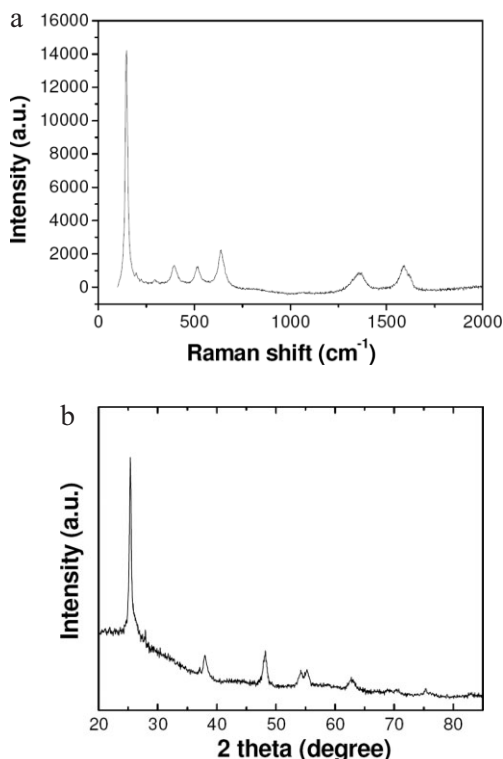


Figure 2. a) A Raman spectrum of a TiO₂-coated VACNT sample corresponding to Figure 1e, and b) the corresponding XRD pattern.

advantages for various optoelectronic applications. The photoelectronic performance of the TiO₂-VACNT coaxial nanowires was thus evaluated by carrying out photocurrent measurements. As seen in Figure 3, the newly observed photocurrent response to a pulsed light beam ($\lambda = 254$ nm, 4 W) is apparently very fast with good repeatability. The strong photocurrent response was observable even when the measurements were deliberately recorded at a temperature as low as -60°C , indicating that a thermal effect is not responsi-

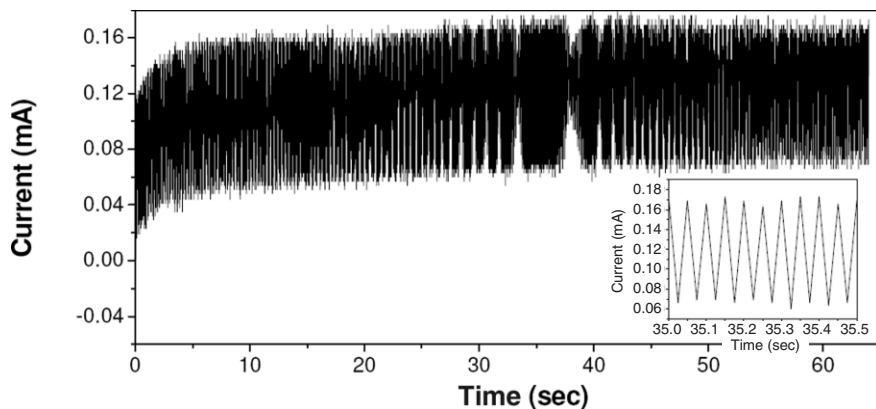


Figure 3. A typical photocurrent response for a TiO₂-VACNT coaxial nanowire film under UV exposure ($\lambda = 254$ nm, 4 W) at room temperature. The inset shows an enlarged view for a small portion of the photocurrent response curve. The sample size is ca. $1\text{ cm} \times 1\text{ cm}$.

ble for the photocurrent generation. This, together with the absence of photocurrent response in control experiments on the pure VACNTs, TiO₂ nanotubes, or TiO₂ nanomembranes, indicates, most probably, a direct electron/hole injection between the TiO₂ layer and the underlying metallic VACNTs through photoexcitation of TiO₂.^[23]

The observed photocurrent response prompted us to use the photoexcited electrons from TiO₂ to deposit various metal nanoparticles (e.g. Au, Ag, Pd, and Pt) onto the TiO₂ nanostructures produced in this study without involving any reducing agent, as in the case of deposition of metal nanoparticles onto CNT structures by our previously reported surface-enhanced electroless deposition (SEED) method.^[24,25]

Unlike the SEED method, however, the photoexcitation method described below can deposit metal nanoparticles onto a TiO₂ surface from a metal salt solution by directly transferring the photoexcited electrons to reduce the metal ions. Like most other photoprocesses, the photoexcitation method developed in the present study should also enable us to deposit metal nanoparticles onto TiO₂ surfaces, in either a nonpatterned or patterned form. Figure 4a shows a typical SEM image of a TiO₂-VACNT coaxial nanowire film (see Fig. 1e) after having been photoexposed ($\lambda = 254$ nm, 4 W) through a photomask (e.g. a TEM grid consisting of hexagonal windows) in an aqueous solution of AgNO₃ (5 mM) for 1 min, which shows a close replication of the mask structure with the newly formed Ag nanoparticles well registered within the hexagon region. An enlarged view of the squared area in Figure 4a is given in Figure 4b, which shows homogeneously packed nanoparticles with diameters of ca. 300 nm. Some relatively larger white spots seen in Figure 4a can be attributed to big Ag clusters formed from small particles as Ag nanoparticles are known to be susceptible to self-assembling.^[26]

Similarly, various other metal nanoparticles can also be region-specifically deposited onto the TiO₂-coated CNT substrate, as exemplified in Figure 4c in which Au nanoparticles were deposited in lines by carrying out the photoexcitation process in an aqueous solution of HAuCl₄ (1.6 mM) through a TEM grid consisting of linear windows. As can be seen in the inset of Figure 4c, nanoparticles with diameters of ca. 250 nm were clearly evident around the individual TiO₂-VACNT coaxial nanowires. The corresponding energy-dispersive X-ray (EDX) spectroscopy spectrum in Figure 4d shows the presence of Au, Ti, O, C, and Si, arising from the newly deposited Au nanoparticles, the TiO₂-coated CNTs, and the silicon substrate.

In summary, we have electrophoretically deposited TiO₂ onto VACNTs and prepared various novel TiO₂ nanostructures (e.g. nanotubes, nanomembranes) by removal of the CNT template through air oxidation at high tempera-

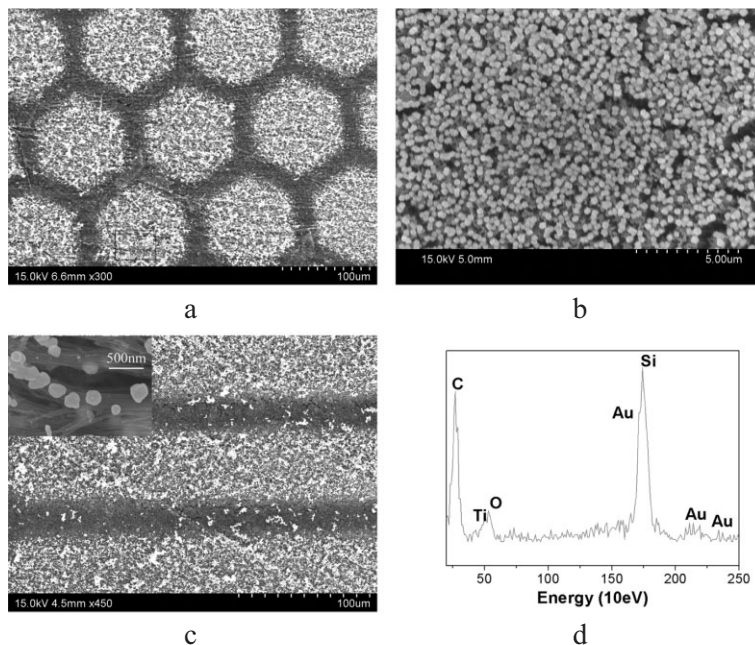


Figure 4. a) An SEM image of the top surface of a TiO₂-VACNT coaxial nanowire film after UV irradiation ($\lambda = 254$ nm, 4 W for 1 min) through a TEM grid with hexagonal windows as the physical mask in an aqueous solution of AgNO₃ (5 mM). b) An enlarged view of the squared area in (a). c) An SEM image of the top surface of a TiO₂-VACNT coaxial nanowire film after UV irradiation ($\lambda = 254$ nm, 4 W for 1 min) through a TEM grid with linear windows as the physical mask in an aqueous solution of HAuCl₄ (1.6 mM). The inset shows individual TiO₂-VACNT coaxial nanowires taken out from the sample corresponding to (c). d) The corresponding EDX spectrum of the gold nanoparticle-deposited TiO₂-VACNT coaxial nanowires. Note that the photoexcitation deposition of metal particles occurs with TiO₂ films even without the underlying CNTs.

tures (typically, 600 °C). The TiO₂-VACNT coaxial nanowires thus prepared were demonstrated to show novel fast photocurrent responses. This, together with the newly discovered photoexcitation-induced patterned/nonpatterned metal-nanoparticle deposition onto the TiO₂-VACNT coaxial nanowires and other TiO₂ nanostructures, represents a significant advance in the development of new photoelectronic nanomaterials for various device applications, ranging from photodetectors to photocatalysts and to many other optoelectronic systems. Owing to the generic nature of the electrophoresis and photoprocesses, the methodologies developed in this study for the fabrication of TiO₂ nanostructures and their derivatives could be readily transferred to the development of various novel photoelectronic nanomaterials based on many other metal oxides.

Experimental

SEM was performed on a Hitachi S-4800 high-resolution scanning electron microscope. An energy-dispersive EDX detecting unit was used for the elemental analysis. TEM images were taken on a Hitachi H-7600 transmission electron microscope. X-ray photoelectron spectroscopy measurements were performed on a VG Microtech ESCA 2000 unit using monochromatic MgK α radiation at 300 W. XRD patterns were recorded on a Rigaku X-ray diffractometer by using a reflection method. Raman spectra were measured on an Invia microscopic Raman spectrometer. UV-vis spectra were measured with a Perkin-Elmer Lambda 900 UV/VIS/NIR spectrometer. UV illumination was provided by using a handheld UV lamp

(UVP UVG-11) with a wavelength of 254 nm and 4 W, while the photocurrent measurements were performed on an eDAQ potentiostat electrochemical analyzer.

Received: September 25, 2006
Revised: December 5, 2006
Published online: April 5, 2007

- [1] G. Dagan, M. Tomkiewicz, *J. Phys. Chem.* **1993**, *97*, 12651.
- [2] C. Hariharan, *Appl. Catal. A* **2006**, *304*, 55.
- [3] Y. X. Li, W. Wlodarski, K. Galatsis, S. H. Moslih, J. Cole, S. Russo, N. Rockelmann, *Sens. Actuators* **2002**, *83*, 160.
- [4] C. H. Lin, C. F. Lai, T. S. Ko, H. W. Huang, H. C. Kuo, Y. Y. Hung, K. M. Leung, C. C. Yu, R. J. Tsai, C. K. Lee, T. C. Lu, S. C. Wang, *IEEE Photonics Technol. Lett.* **2006**, *18*, 2050.
- [5] See, for example: J. Song-Rim, R. Vittal, K. Kang-Jin, *Langmuir* **2004**, *20*, 9807.
- [6] L. Qu, Y. Zhao, L. Dai, *Small* **2006**, *2*, 1052.
- [7] See, for example: a) A. Matsumoto, K. Tsutsumi, K. Kaneko, *Langmuir* **1992**, *8*, 2515. b) M. Langlet, A. Kim, M. Audier, J. M. Herrmann, *J. Sol-Gel Sci. Technol.* **2002**, *25*, 223.
- [8] See, for example: a) X. Zhang, M. Zhou, L. Lei, *Carbon* **2005**, *43*, 1700. b) B. Tryba, A. W. Morawski, M. Inagaki, *Appl. Catal. B Environ.* **2003**, *41*, 427. c) W. H. Shen, Y. F. Zhu, X. P. Dong, J. L. Gu, J. L. Shi, *Chem. Lett.* **2005**, *34*, 840. d) Z. K. Liu, Y. L. He, F. Li, Y. H. Liu, *Environ. Sci. Pollut. Res. Int.* **2006**, *13*, 328. e) P. F. Fu, Y. Luan, X. G. Dai, *Trans. Nonferrous Met. Soc. China* **2006**, *16*, 965. f) R. S. Yuan, R. B. Guan, J. T. Zheng, *Scrip* **2005**, *52*, 1329. g) J. Matos, J. Laine, J. M. Hermann, *J. Catal.* **2001**, *200*, 10. h) T. Tsumura, N. Kojitani, H. Umemura, M. Toyoda, M. Inagaki, *Appl. Surf. Sci.* **2002**, *196*, 429.

- [9] *Carbon Nanotechnology: Recent Developments in Chemistry, Physics, Materials Science and Device Applications*, (Ed. L. Dai), Elsevier, Amsterdam, **2006**.
- [10] A. Jitianu, T. Cacciaguerra, R. Benoit, S. Delpeux, F. Beguin, S. Bonnamy, *Carbon* **2004**, *42*, 1147.
- [11] See, for example: a) T. Kasuga, M. Hiramatsu, A. Hoson, T. Sekino, K. Niihara, *Langmuir* **1998**, *14*, 3160. b) T. Kasuga, M. Hiramatsu, A. Hoson, T. Sekino, K. Niihara, *Adv. Mater.* **1998**, *10*, 3160. c) S. Uchida, R. Chiba, M. Tomiha, N. Masaki, M. Shirai, *Electrochemistry* **2002**, *70*, 418. d) T. Kasuga, *Thin Solid Films* **2006**, *496*, 141.
- [12] See, for example: a) X. S. Peng, J. P. Wang, D. F. Thomas, A. Chen, *Nanotechnology* **2005**, *16*, 2389. b) X. S. Peng, A. C. Chen, *Zesz. Nauk. Politech. Bialostockiej Mat. Fiz. Chem* **2004**, *14*, 2542. c) W. Y. Wang, Y. Ku, *J. Membr. Sci.* **2006**, *282*, 342. d) C. Wang, P. Xu, Z. Q. Mao, L. S. Wang, K. Y. Ge, J. M. Xu, *Rare Met. Mater. Eng.* **2006**, *35*, 1432.
- [13] a) L. Dai, A. W. H. Mau, *J. Phys. Chem. B* **2000**, *104*, 1891. b) L. Dai, "Intelligent Macromolecules for Smart Devices: From Materials Synthesis to Device Applications", Springer, Berlin, **2004**.
- [14] Q. Chen, L. Dai, M. Gao, S. Huang, A. W. H. Mau, *J. Phys. Chem. B* **2001**, *105*, 618.
- [15] a) L. Dai, A. Patil, X. Gong, Z. Guo, L. Liu, Y. Liu, D. Zhu, *Chem-PhysChem* **2003**, *4*, 1150. b) P. He, L. Dai, *Chem. Commun.* **2004**, 348.
- [16] a) M. Gao, S. Huang, L. Dai, G. Wallace, R. Gao, Z. Wang, *Angew. Chem. Int. Ed.* **2000**, *39*, 3664. b) M. Gao, L. Dai, G. Wallace, *Electroanalysis* **2003**, *14*, 1089.
- [17] S. J. Limmer, S. Seraji, Y. Wu, T. P. Chou, C. Nguyen, G. Cao, *Adv. Funct. Mater.* **2002**, *12*, 59.
- [18] S. Huang, L. Dai, A. W. H. Mau, *J. Phys. Chem. B* **1999**, *103*, 4223.
- [19] Y. Yang, S. Huang, H. He, A. W. H. Mau, L. Dai, *J. Am. Chem. Soc.* **1999**, *121*, 10832.
- [20] S. J. Limmer, T. P. Chou, G. Z. Cao, *J. Mater. Sci.* **2004**, *39*, 895.
- [21] M. P. Moret, R. Zallen, D. P. Vijay, B. S. Desu, *Thin Solid Films* **2000**, 366, 8.
- [22] B. L. Abrams, J. P. Wilcoxon, *Crit. Rev. Solid State Mater. Sci.* **2005**, *30*, 153.
- [23] X. Feng, J. Zhai, and L. Jiang, *Angew. Chem. Int. Ed.* **2005**, *44*, 5115.
- [24] L. Qu, L. Dai, *J. Am. Chem. Soc.* **2005**, *127*, 10806.
- [25] L. Qu, L. Dai, E. Osawa, *J. Am. Chem. Soc.* **2006**, *128*, 5523.
- [26] L. Qu, L. Dai, *J. Chem. Phys.* **2005**, *122–123*, 13985.